2. Sources of medical images and their general characteristics

2.1. X-ray images

In 1895, the German physicist Wilhelm Roentgen (Fig. 2.1.a) noted that a cathode tube exposes paper coated with a barium compound placed at some distance away. The tube emitted radiation, unknown at that time, which caused the plates to get exposed. Roentgen named that radiation "X rays". His discovery, for which he received the Nobel Prize in 1901 (Fig. 2.1.b and 2.1.c) caused a revolution in medicine, for the first time making it possible to look inside the human body without breaking its integrity, in a way now referred to as noninvasive [2].

Fig. 2.1. Wilhelm C. Roentgen and a copy of his 1901 Nobel Prize certificate (source Internet)

This technology was subsequently improved by constructors of machines offered to hundreds of radiology practices. The scale of these improvements can be assessed by comparing the historical image from the first ever x-ray examination of a human being (the image of Wilhelm Roentgen's wife's hand – Fig. 2.2.a) with a similar photograph generated by a modern X-ray machine – Fig. 2.2.b.

Fig. 2.2. A historic photograph of Roentgen's wife's hand (left) contrasted with a present-day X-ray photograph (right) (source Internet)

X-ray photography, regardless of its shortcomings (X rays, like any ionizing radiation, are harmful to human health), has become a diagnostic technique widely used until the present. This is why the discussion of various medical imaging techniques presented in this book has to start with X-ray photography, which will occupy the entire first subsection of the second chapter [2].

X-rays are generated in a special tube (Fig. 2.3) in which a beam of electrons accelerated by high voltage hits a metal disk and as a result of the rapid deceleration its kinetic energy is transformed into quanta of emitted X-rays, whose ability to penetrate the human body is the greater the higher the voltage accelerating the electrons in the tube. Electrons hitting the disk make it very hot, so it either has to be cooled on the inside (usually with water) or spun so that electrons hit a new spot while the spot struck previously cools down.
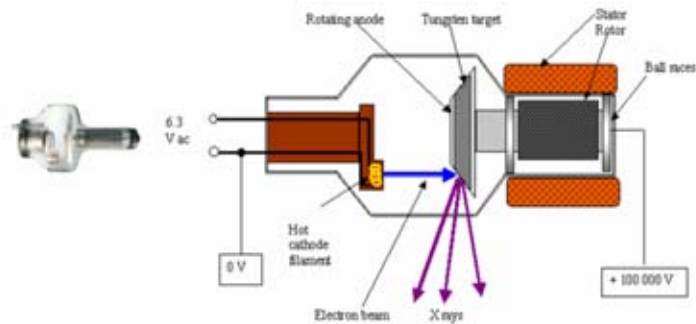

Fig. 2.3. An image and a diagram of an X-ray tube

One feature of X-rays, like of any electromagnetic radiation, is that a certain part of them is weakened after they pass through tissues. This weakening is the result of their interaction with the tissues, and the scale of it depends on the type of tissue they passed through. The intensity of X-ray radiation also depends on the distance and decreases along with the square of the distance. Interactions of X-rays with matter can be divided into three types:

- **The Compton effect** – the electron lying in the trajectory of the beam absorbs some of the energy of the photon forming a part of the beam and changes the direction in which that photon is traveling. As a result, the photon changes its direction and its energy is reduced (Fig. 2.4.a).
- **Rayleigh scattering** – a flexible (i.e. free of energy losses) scattering of photons over atoms which do not absorb energy. Unlike in the Compton effect, the photons of the beam do not lose any energy, only change their direction (Fig. 2.4.b).
- **The photoelectric effect** – a photoelectron is ejected by a photon of the beam. The photon is absorbed by the atom (Fig. 2.4.c).
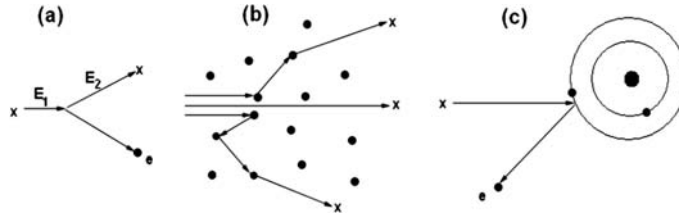
Fig. 2.4. Physical effects that occur when X-rays pass through matter (the patient's body). Described in the text

The main factor causing the weakening of the beam is the Compton effect. The three above effects can be characterized collectively by the following absorption equation (for a uniform medium):

$$I = I_0 e^{-\mu x}$$

where I_0 is the initial intensity of radiation, x is the thickness of the layer through which the beam passes, and μ is the specific absorbance of the substance (its radiodensity). The μ radiodensity depends on the type of substance through which the radiation passes. It is expressed using the Hounsfield scale, presented in Figure 2.5. The reference value (of 0) on that scale is the X-ray absorption by water (which is the main component of all tissues and organs of living organisms). Substances with X-ray absorbance weaker than water (e.g. the air in the lungs) have negative Hounsfield values, down to –1,000 Hounsfield units for light gases. Conversely, substances with X-ray absorbance greater than water (e.g. bones) have positive values, up to +1,000 which is assigned to very hard and dense bones.

X-rays ionize matter and cause luminescence, they also interact with photographic emulsions and semiconductor radiation detectors currently used for X-ray recording and imaging. Unfortunately, these rays also ionize biological tissues, damaging them and potentially leading to many serious diseases. So regardless of the diagnostic benefits accruing from every extra X-ray image, the number of examinations should be limited to the indispensable minimum in order to protect the patient's body from the consequences of exposure to this harmful radiation.

Figure 2.5 shows that tissues of which various organs of the human body are built have μ radiodensities varied enough, so that when X-rays pass through the examined patient's body, depending on the organs and tissues lying along the path from the radiation source to the place of its recording, different levels of energy reach the film coated with the appropriate photosensitive emulsion or the X-ray detector placed on the other side of body. This is the basic effect used in this type of imaging: in the places to which radiation traveled through tissues with a low value on the Hounsfield scale, the film darkens or the CCD detector is excited, while places located behind e.g. parts of the skeleton receive little radiation energy, so light spots are left on the film or electronic detectors return a weak signal (Fig. 2.6).
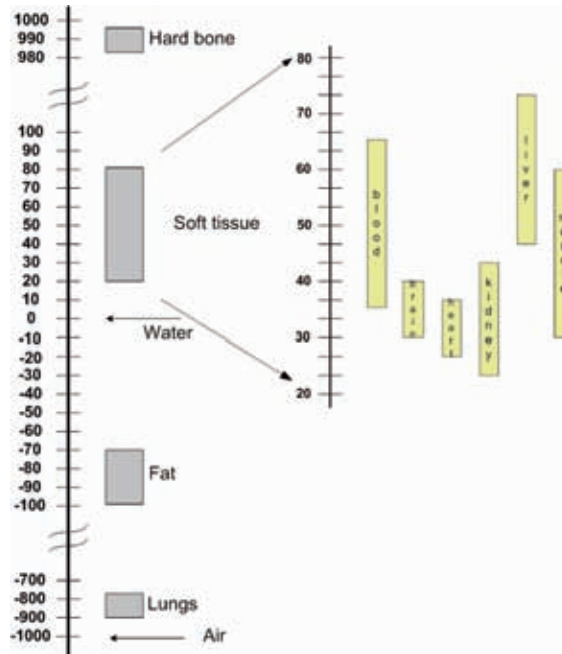
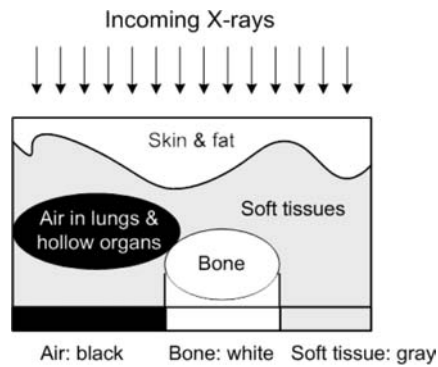**Fig. 2.5.** The Hounsfield scale used in x-ray diagnostics

Fig. 2.6. The principle behind the imaging of various tissues in X-ray diagnostics

This suggests that what you see on the acquired medical image are shadows of the organs through which the radiation had to pass, and the more cohesive and dense the organ, the brighter its image (cf. Fig. 2.2.).

It is sometimes said that the X-ray image is the *negative* of the picture of the examined organs, but regardless of the ease with which today's digital radiography could invert grey levels to obtain a positive image, no one does this, as all the

traditional methods of interpreting X-ray images used by physicians for years apply to images in the form of negatives.

Fig. 2.7. An example of a modern X-ray machine (source Internet)

In practical medical diagnostics, X-ray images are produced by X-ray machines (Fig. 2.7), which may have been improved compared to the historical Roentgen machine, but their operating principle has not changed. They contain at least one X-ray tube, a high voltage generator supplying that tube and devices recording the intensity of radiation after its passage through the patient's body. In less expensive machines, radiation intensity is recorded by a special set of electronic CCD detectors or (in older solutions) on a special photographic plate. Nowadays, the radiation is not recorded directly, but its intensity is measured and then converted into an image. This makes more details visible in the image (Fig. 2.8).
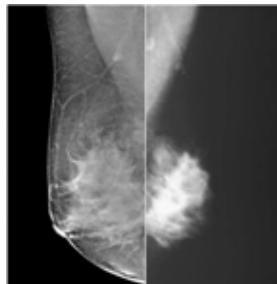

Fig. 2.8. An image produced using modern methods of X-ray intensity measurement and computer-aided imaging (left) compared with an image of the same organ (female breast) recorded on a traditional plate

Contemporary X-ray machines are computer controlled, so examination parameters can be automatically tailored to the patient. They can produce X-ray photographs as well as images for the instant evaluation by doctors. There are also machines for specialized examinations, such as:

- mammography (Fig. 2.9.),
- dental photographs (Fig. 2.10),

- chest and heart diagnostics (Fig. 2.11),
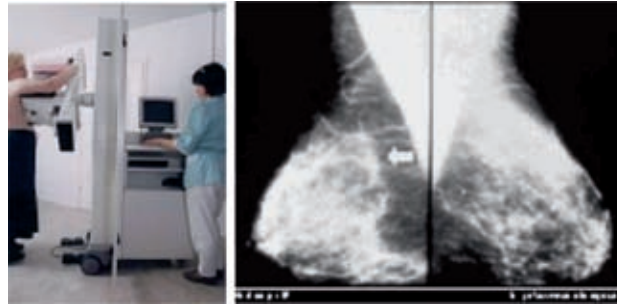- skeletal system diagnostics (Fig. 2.12).

Fig. 2.9. Specialized X-ray examination: mammography (source Internet)

Fig. 2.10. Dental radiography (source Internet)

Fig. 2.11. Lung and heart X-ray examinations (source Internet)

Fig. 2.12. Bone X-ray examination (source Internet)

The radiological image can be recorded and presented in many ways. The following ways of recording these images are used:

- Traditional X-ray photographs obtained using classical photographic plates;
- Digital computer radiology;
- Systems which allow the functions of the organ to be recorded
- CAT scanning (described further down in the chapter).

The improvements in X-ray technology have, however, led to the following problem. Modern detectors can measure the intensity of X-rays so precisely that differences in the radiodensity of single Hounsfield units or even their fractions can be imaged. This means that the digital X-ray image generated in the computer memory consists of pixels represented by between 12 and 16 bits, so the brightness of those points can take one of 4,096 or even 65,536 discrete levels. However, the image is displayed using devices that can only differentiate 256 levels of brightness (or grey levels), while the physician interpreting the image can only differentiate some 60 grey levels with his/her eyesight. This means that due to the limitations of human perception, the proportion of the information that the medical doctor can use to the information obtained by X-ray imaging is like 1:1,000. This is one of the crucial arguments supporting the broad application of computer analysis of medical images to help the physician interpret them, but the problem of the narrow perception range of the human eye also has to be solved somehow.

The problem is most frequently solved by providing a "window" functionality which allows the person to select and see only that fragment of the variability interval of brightnesses expressed on the Hounsfield scale which we believe carries information useful for the diagnostic problem analysed at the time. If we have reasons to believe that the relevant organs and tissues are represented by pixel values from the $[W_1, W_2]$ interval isolated from the complete Hounsfield scale, then we can "cut" that interval using the computer and then rescale it to 256 grey levels. The decision on what W_1, W_2 threshold values to select depends on the physician, as this selection will determine which fragments of the examined body will be captured. It is customary to define W_1, W_2 using the L and W figures, where L is the middle level of the "window", while W is the window width. Examples of the *L* and *W* values used in examinations are: window width $W = 300$–600 HU for soft tissues and 800–1600 HU for lungs, window level $L = 0$–30 HU or 30–60 HU for soft tissues and –500–700 HU for lungs. Fig. 2.13 shows what the same X-ray image looks like when different L and W values are chosen.

X-ray images of the same parts of the body may look different depending on how "hard" the radiation generated was. The hardness or penetrating ability of X-rays is adjusted by selecting the voltage accelerating electrons in the tube (cf. Fig. 2.3). As the most frequent examinations made using this technique are skeleton photographs, the most popular voltage is about 70 kV, since at that energy the quanta of X-rays support the best imaging of particular parts of the skeletal system. A similar range of voltages is used to obtain dental images of teeth, while lower voltages of some 50 kV are used to examine the organs in the chest. For soft

tissue X-rays (e.g. mammography), a lower interval of voltages is used: 15 kV to 18 kV.
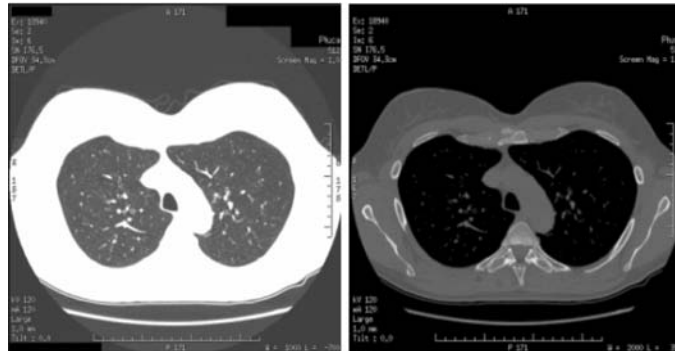

Fig. 2.13. The same X-ray image when different L and W values are chosen: on the left L = –700 HU, W = 1000 HU, on the right L = 350 HU, W = 2000 HU

In some cases, to get the right information about the morphology or the structure of an organ, the patient is given a contrast medium. This medium must have a radiodensity much different from that of the surrounding tissues. It fills the appropriate body cavities (e.g. the inside of the stomach – Fig. 2.14) to give their more precise view.

Fig. 2.14. Using a contrast medium for stomach imaging

Imaging the same organ in the same position before and after administering the contrast medium offers interesting opportunities. Subtracting these two images from one another yields an image in which the anatomic details filled with the contrast can be seen (Fig. 2.15). All other anatomic details which did not differ in the two pictures are removed almost completely as a result of the subtraction (*almost* and not completely because you can never get exactly the same position and the same exposure conditions of the organ before and after the contrast was administered). This examination technique is most frequently used to image various vessels (e.g. blood vessels), which is why it is called *angiography*. As this method of discovering anatomic structures is based on

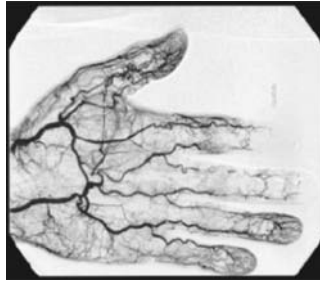the mathematical operation of subtracting, the adjective *subtraction* is added to the name.

Fig. 2.15. The result of subtraction angiography. Described in the text

2.2. CT images

Apart from magnetic resonance, computed tomography (CT) represents one of the main noninvasive diagnostic techniques used in contemporary medicine. Its popularity is driven both by technological progress yielding subsequent generations of apparatuses with even better parameters of the acquired image, also in the form of 3D reconstructions, and by even faster computers used for the mathematical processing of the measurement data collected [25].

A CT examination consists of probing the patient many times with an appropriately shaped beam of X-rays (Fig. 2.16). When the beam passes through the examined tissues it gets weaker, and its final intensity is measured by the detector. The weakening of the beam (the absorption of radiation) along the path to the detector depends on the type of substance that it penetrates, but for a single probe we get the summary effect of beam weakening by all tissues that it encounters along its path. It is possible to reconstruct the radiation absorption by a specific point on the cross-section of the patient's body as the CT apparatus collects the results of many such images made by beams running in different directions and intersecting many times at different points inside the patient's body. By analyzing the signal recorded by detectors for many such beams, it is possible to calculate the degree of radiation absorption by particular fragments of the examined patient's body, called voxels (Fig. 2.16) through solving the appropriate systems of equations.

On the basis of the results obtained, it is possible to precisely identify the examined tissues and to reconstruct the shapes of organs by making the appropriate calculations. The identification is difficult, as it requires both many measurements and complicated mathematical operations leading to the reconstruction of the spatial structure of the object.
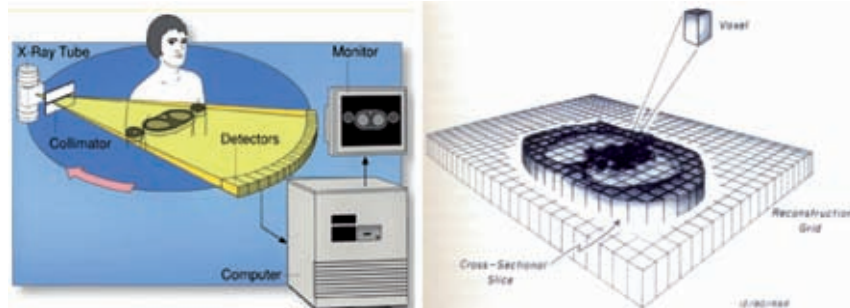
Fig. 2.16. The operating principle of a CT apparatus (source Internet)

The main contribution to the development of CT was made by Godsfrey Hounsfeld (Fig. 2.17), who discovered in 1970 that measurements of the absorption of X-rays allow tissue density to be determined. The technique was first used in 1971, but with only moderate success (see Fig. 2.17).
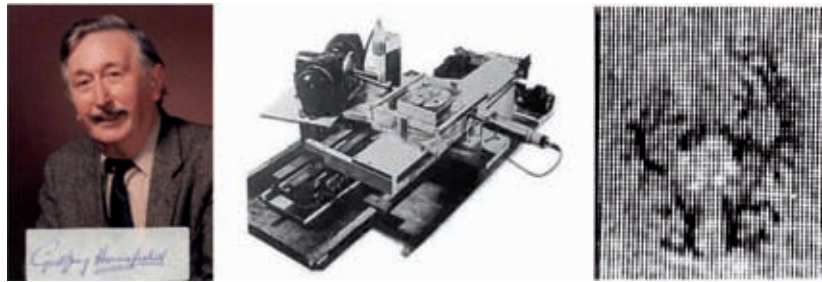

Fig. 2.17. Godfrey Newbold Hounsfield, his CT apparatus and the first CT image (source Internet)

However, the CT technique was gradually improved, mainly as it was not subject to the limitations of traditional X-ray techniques. In a CT image, organs do not obscure one another, so it is possible to make a precise image of the inside of the brain, for example, regardless of the massive shield of the scull behind which it is hidden. In addition, in CT, the density of particular tissues can be calculated so precisely that it is possible to make differentiations absolutely impossible by any other method: for example, congealed blood can be distinguished from flowing, allowing the extent of a stroke to be determined.

Subsequent generations of CT apparatuses could acquire the necessary images within shorter and shorter times while maintaining the principle of a multidirectional probing inside the human body (Fig. 2.18, 2.19).
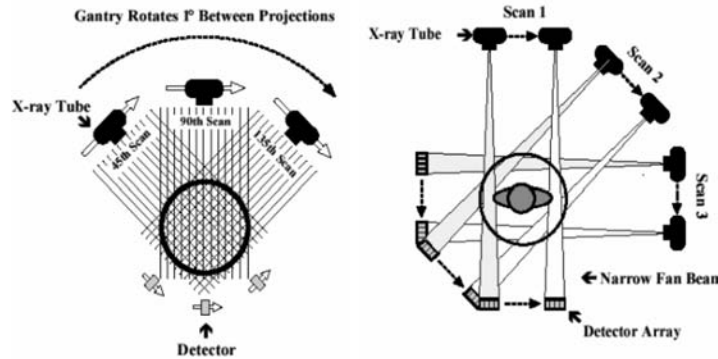
Fig. 2.18. The transition from the first to the second generation of CT apparatuses meant replacing one radiation beam with a whole fan of them and one detector with an array of detectors. This cut the image production time
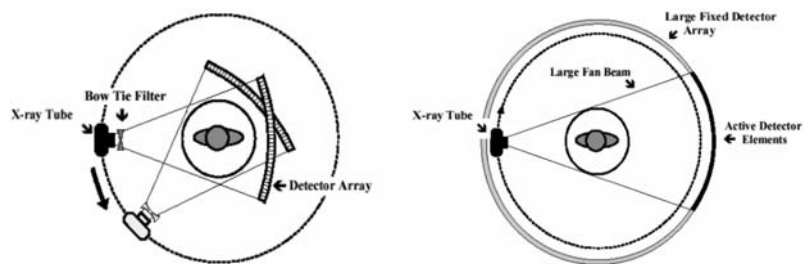

Fig. 2.19. Further progress was achieved mainly by adding more and more detectors, which finally filled the entire ring in the 4th generation CT apparatuses

An innovation in the CT technology was the introduction of a CT apparatus that spun the X-ray tube in a spiral around the patient (Fig. 2.20). The first such examination was made in 1989. The move from the sequential to the spiral technique made it possible to image the human body along any plane. For this reason, spiral computed tomography is now referred to as the volumetric CT or 3D CT. The current CT apparatuses used in medicine allow between one and sixty-four layers to be recorded during one revolution of the tube. This cuts the examination time, reducing the radiation dose.

Computed tomography made it possible to directly assess the brain and other structures inside the skull, which were previously practically out of bounds for radiological examination. In addition, CTs made it possible to determine if these structures had not been shifted. CTs enable the diagnosing specialists to detect many diseases, e.g. tumors and haematomas, which were previously difficult to identify using X-rays. Even though diagnostic capabilities of CT are poorer than those of magnetic resonance, CT is a very popular examination as it is easily available and the acquired images are very legible (Fig. 2.21).
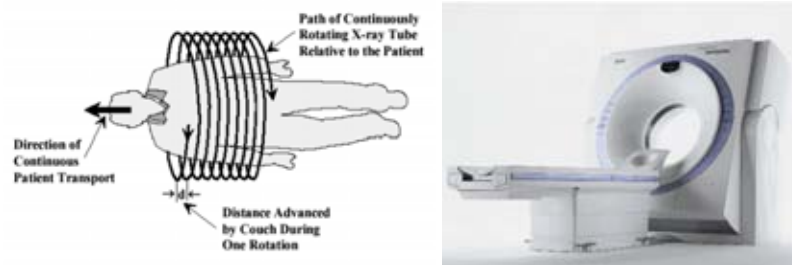
Fig. 2.20. Spiral CT. The operating principle and a view of the apparatus (source Internet)

Fig. 2.21. Images produced by CT examinations are of very high quality

The key components of a CT apparatus are shown in Fig. 2.22. The computed tomography apparatus consists of bed on which the examined patient lies, the gantry (a ring-shaped element containing X-ray tubes and radiation detectors) and a computer. Data collected by detectors, including information about the positions of the tube and detectors, is analyzed by the computer to reconstruct the image. In spiral tomography, the bed can move relative to the gantry along its axis of symmetry.
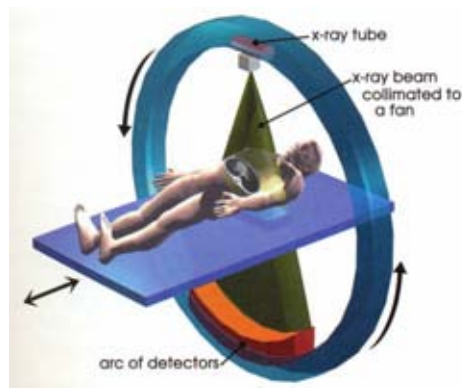

Fig. 2.22. Main structural elements of the CT apparatus (source Internet)

The part of the patient's body to be scanned is divided into layers (Fig. 2.23), every one of which consists of volume elements called voxels (volumetric pixels) (see Fig. 2.16). Cross-sections may lie in three planes (Fig. 2.24).
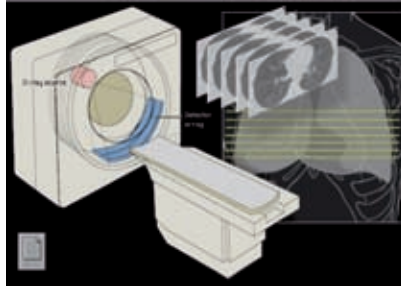

Fig. 2.23. A CT examination produces a series of images representing subsequent cross-sections of the examined fragment of the patient's body (source Internet)

Fig. 2.24. The CT apparatus can produce images of body cross-sections along different planes (source Internet)

A single cross-section, 0.75 mm – 10 mm thick, is a matrix of voxels subsequently represented by pixels of the produced image. The matrix size for images used in this publication is 512×512 voxels (pixels). The resolution of a voxel is about $0.5 \times 0.5 \times 0.6$ mm. In general, reducing the volume of a voxel improves image quality, but brings about an increase in the radiation dose.

Series of cross-sections obtained by a CT examination can be analyzed as sequences of images on the basis of which the physician formulates the diagnosis and prescribes the treatment, but a more attractive functionality is offered by the ability of the computer to reconstruct a spatial image of the organ analyzed (Fig. 2.25).
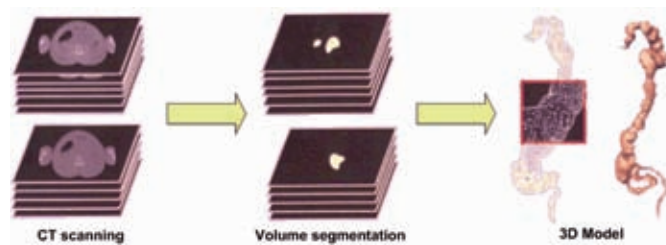

CT scanning   Volume segmentation   3D Model

Fig. 2.25. The principle for creating a three-dimensional model based on a series of cross-sections from a CT scan

Tissue densities calculated by the CT apparatus are expressed on the Hounsfield scale discussed in the previous subsection (as part of the discussion of X-ray image characteristics). For the human body, these values range from –1000 HU to 1000 HU and cannot be precisely shown to a person who would like to assess these images visually. This is why for CT images, the selected Hounsfield values range is also replaced with the set (0, 1, ..., 255). In this examination, it is also customary to define the W_1, W_2 limits and then represent the middle level of the interval with the L value and the width of the window with the W:

$$L = \frac{W_1 + W_2}{2}, \ W = W_2 - W_1.$$

The right selection of the L and W values used in the examination not only determines what is visible in the image (Fig. 2.26) but also makes it possible to control the subjective impression received by the physician analyzing the image (Fig. 2.27).
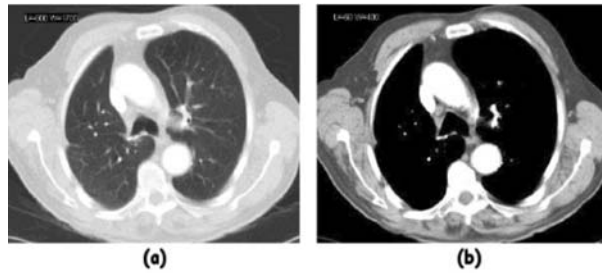

Fig. 2.26. Image (a) obtained for L = –600, W = 1700 shows much more details, while in image (b) produced at L = 50, W = 400 many items are not visible, but it is easier to focus on the distinguished objects

CT images showing the same anatomical structures of different patients can be compared more easily by applying a grid which shows individual deformations to be applied to the image of the examined patient to enable his/her comparison with the reference image. This technique is discussed in one of the subsequent chapters.
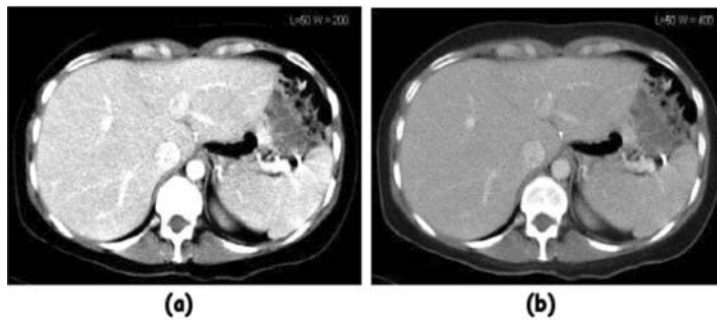

Fig. 2.27. Using a wider window reduces the contrast of the image, so it appears less noisy (image (a) L = 50 and W = 200, image (b) at L = 50 and W = 400)

2.3. NMR images

One of the newest and best methods of diagnostic imaging is the magnetic resonance (MR) technique, which uses the phenomenon of nuclear magnetic resonance (NMR) [17]. Since the word "nuclear" is tainted by unpleasant associations with atom bombs, Chernobyl and radioactivity, this method is sometimes also called Magnetic Resonance Imaging (MRI). However, MRI methods us atomic nuclei, and more precisely the fact that some of them have a spin, so they exhibit a magnetic moment (Fig. 2.28). This technique was first used for clinical examinations in 1982.
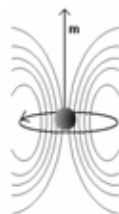

Fig. 2.28. NMR imaging makes use of the spin of certain atomic nuclei, which gives them a natural magnetic moment

Magnetic resonance mainly uses hydrogen analysis, which means that the generation of electromagnetic radiation by hydrogen atom nuclei (protons) in the organism is analysed. This is because these nuclei return a very clear signal when they are properly magnetically excited and because hydrogen is widely present in the human body, for instance in the water which constitutes one of the main building blocks of our organisms.

Another element whose nuclei exhibit a non-zero spin, and can therefore be used for nuclear magnetic resonance imaging, is phosphorus. The signal obtained from phosphorus nuclei is more difficult to receive and interpret, but phosphorus plays a key role in the activity of live tissues and whole organs. Phosphorus atoms are present in molecules of one important chemical compound: Adenosine 5'-triphosphate (ATP – Fig. 2.29). This substance is the main source of energy for all biological processes, so by using NMR to find out where ATP molecules are situated in the examined organ we can also discover which parts of the organ are active, and which are less active. This is of major importance for attempts to link medical images not just to the morphology of specific organs, but also to their function.
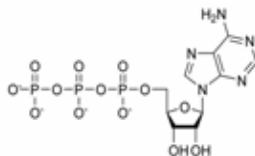

Fig. 2.29. ATP is a chemical compound whose location can be determined using the NMR

Magnetic resonance is a method for visualizing internal organs of a human (or another biological) being in which the image is constructed in the computer as a result of acquiring and recording a physical signal (an electromagnetic wave of a radio frequency) generated by the organ itself. Consequently, this imaging technique is dramatically different from the previously discussed X-ray examinations (traditional or tomography), in which the source of the signal is an external tube emitting X-rays. In X-ray examinations, the organs are "lit up" with external radiation, and then you view their shadows. In NMR, the organs "shine" themselves, the source of that radiation being the atomic nuclei of elements making up the molecules of which organs are built.
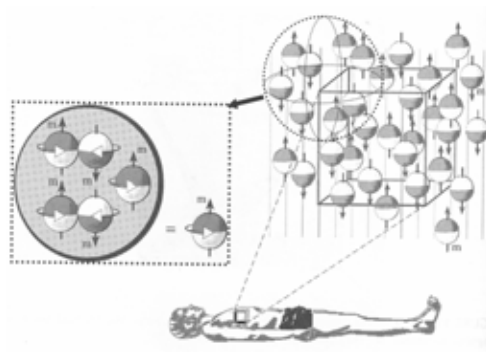

Fig. 2.30. An external magnetic field aligns nuclear spins inside the patient's body (source Internet)

For these natural atoms to start "shining", they have to be appropriately excited. NMR uses a strong magnetic field for imaging. This field causes the nuclei of atoms in the patient's body to be aligned and spatially oriented (Fig. 2.30), so when an external impulse comes to excite them, they respond with a "harmonious tune", giving a clear and easily recordable signal revealing where they are more abundant, and where less. MR apparatuses use permanent, super-conducting and resistance magnets to generate that aligning magnetic field. These magnets differ in the structure and intensity of the field they emit. The magnetic field intensity determines diagnostic capabilities of the MR apparatus: for spectroscopy, quick vascular examinations or functional examinations you need an apparatus with a high field intensity. In medicine, MR apparatuses with the magnetic field intensities ranging from 0.1 to 3.0 Tesla are used.

The key element of the magnetic resonance tomograph (Fig. 2.31) is the chamber in which the examined patient lies [17]. The chamber is inside the main magnet generating the external (to the patient's body) magnetic field B_0 to align the magnetic moments of hydrogen (and phosphorus, as mentioned above) atoms. These aligned magnetic moments of nuclei of all atoms make up the M magnetization vector generated by the entire examined sample. In order to make it uniform, correcting coils which induce an additional magnetic field compensating the non-uniformities of the B_0 field are used. The effect of the linear field

change (gradient), fundamental for NMR examinations, is obtained by using additional gradient coils. On top of this, you need coils which force the "hits" of the external magnetic field, causing the atomic nuclei to resonate, as described above. The device which acquires the signal from the resonating atomic nuclei is the receiving coil with an axis perpendicular to that of the main magnet. This function is frequently provided by the same coils which are used to cause the impulse exciting the resonance. A schematic diagram of the above elements is presented in Figure 2.32.
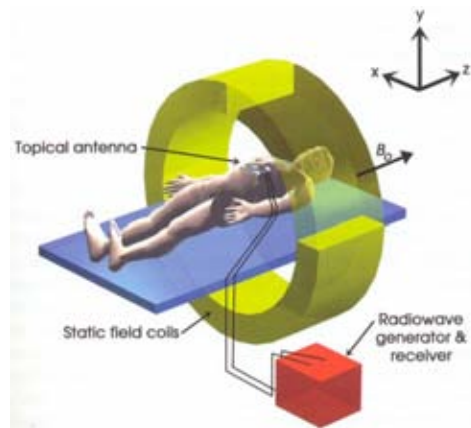

Fig. 2.31. A simplified diagram of an NMR apparatus (source Internet)
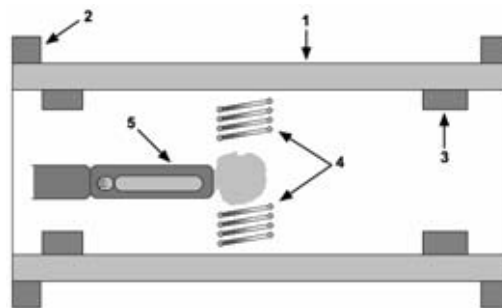

Fig. 2.32. The schematic distribution of particular elements in an NMR apparatus: 1 – main magnet, 2 – correcting coils, 3 – gradient coils, 4 – forcing and receiving coils, 5 – examined patient

The principle of acquiring the signal used for MRI imaging can be summarized as follows. The tissue located in the external B_0 field, which has a specific, defined magnetization M, is exposed to an electromagnetic impulse of a specific, defined frequency (the ω_0 Larmor frequency) whose direction is perpendicular to the direction of M and B_0. In those conditions, a nuclear resonance occurs. It consists in energy absorption by atomic nuclei whose

magnetic moments contributed to the M magnetization. As a result of this phenomenon, the M vector transits to the plane perpendicular to B_0 (the transverse plane) on which it makes rotary (precession) movements at the Larmor frequency (Fig. 2.33). Please note that the relationship between the ω_0 Larmor frequency and the type of nucleus means that an impulse of the right frequency will excite only one type of nuclei.
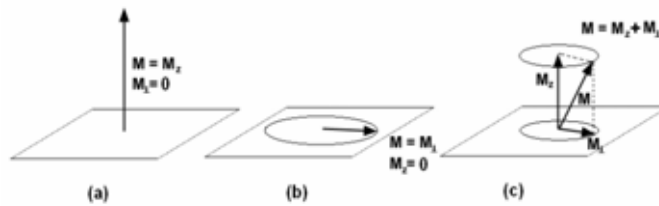

Fig. 2.33. Situation of the magnetization vector of the tissue examined: (a) before exciting, (b) at the moment of excitation, (c) during the relaxation process after the excitation.

An important phenomenon occurs at the level of single atomic nuclei. All the **m** magnetic moments of individual nuclei which make up the M magnetization spin after the excitation, in the transverse plane, at the same frequency (Larmor frequency) and in consistent phases.

The magnetization vector can be split into the sum of two components:

$$\mathbf{M} = \mathbf{M}_\perp + \mathbf{M}_z,$$

where $\mathbf{M}_\perp$ is the transverse magnetization component lying in the plane perpendicular to the B_0 field direction, while $\mathbf{M}_z$ is the longitudinal component parallel to the B_0 direction. Initially (before the excitation), there is no perpendicular component, so $M_\perp = 0$, as transverse components of magnetic moments of individual nuclei are randomly oriented and therefore neutralize one another. On the other hand, in the moment directly after the excitation, $\mathbf{M}_z = 0$ and the magnetization vector lies in the transverse plane.

If the appropriately oriented receiving coil is placed in the vicinity of such an excited tissue, then in accordance with the Faraday's law of electromagnetic induction, alternating current with the frequency of ω_0 will appear in the coil. This is called the free induction decay (FID) signal. The magnitude of this current depends on the value of the magnetization M, and more precisely on the value of its transverse component $M_\perp$, which at the initial moment satfies the equation $M = M_\perp$. The current induced as a result of the magnetic resonance effect constitutes a signal, the knowledge of which allows an image of the examined tissue to be created.

After the impulse which caused the resonance ends, a phenomenon referred to as *the relaxation* occurs (see Fig. 2.33).

Relaxation consists of two independent processes:

1. The M_z longitudinal component of magnetization is restored. This is due to the constant presence of the B_0 external magnetic field.
2. The $M_\perp$ transverse component decays to zero. The disappearance of $M_\perp$ is brought about by two reasons. The first is the non-uniformity of the B_0 magnetic field, the second comes from interactions between the **m** magnetic moments of adjacent nuclei.

The return of the M_z magnetization to its original value and the total decay of the $M_\perp$ value take place within different time scales, characterized by two time-constants T_1 and T_2, respectively referred to as the time of longitudinal relaxation and the time of transverse relaxation (Fig. 2.34). The T_1 parameter is defined as the time needed for M_z to fall to 63% of its initial value (i.e. before the excitation), while T_2 is the time after which 63% of the $M_\perp$ transverse magnetization following the excitation decays.
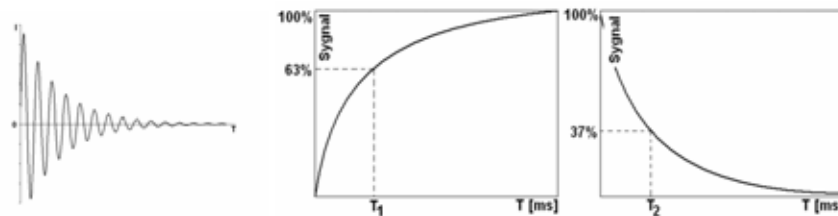

Fig. 2.34. The decay of the transverse magnetization resonance signal during the relaxation (left) and definitions of T_1 and T_2 time-constants (right)

The T_1 and T_2 times range from 0.08 s to 2.5 s for human tissues, depending on the tissue type. The extreme cases are represented by fatty tissue, with short relaxation times, and water, for which T_1 and T_2 are very long. So, for example, T_2 of water is 0.2 s, and T_2 of fat is 0.08 s.

Magnetic resonance diagnostics makes use of not single stimulating impulses, but their sequences. What is important are two time parameters, namely the Time of Repetition (TR) and the Time of Echo (TE), both measured in milliseconds. TR is the time between two subsequent impulses, while TE between the impulse and the maximum signal (current) in the coil (Fig. 2.35).
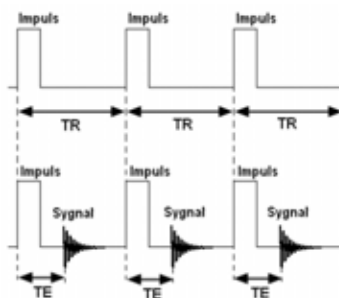

Fig. 2.35. Definitions of TR and TE

TR and TE are apparatus settings, so they can be changed by the operator of the MR scanner. Their right values secure the desired contrast of images obtained from the examination.

Magnetic resonance scanners can be used with three methods of contrasting tissues. The first two use the differences in relaxation times, T_1 or T_2, between different substances of which the human body is made. The third is based on differences in proton densities (PD) of those substances.

For **T1 weighted images** (also called T1 imaging), the important thing is the difference between the rate at which a different tissues recover their $\mathbf{M_z}$ longitudinal magnetization component. As the T_1 time of fat is shorter than the T_1 of water, after the expiry of TR, the value of the longitudinal component of the magnetization vector of fat is greater than of water. As a result, when both magnetization vectors are again "laid" in the transverse plane following the next impulse, the $\mathbf{M}$ magnetization length for fat is longer, the impulse in the coil stronger, and thus the image of this tissue brighter. In this case, the setting that makes it possible to manipulate the contrast is the time of repetition – TR - which determines to what extent $\mathbf{M_z}$ components are recovered. In order to obtain satisfactory imaging, short TR and TE are used.

To produce **T2 weighted images** (T2 imaging, T2 contrasting), the difference in the speed with which the transverse component of magnetization dissipates in various tissues is used. Just as in the previous case, the T_2 transverse relaxation time of fat is shorter than that of water. So if we wait the appropriate TE time after the exciting impulse, we get a relatively strong signal from where water is present and a weak signal (or none at all) from fatty tissue. Consequently, in T2 imaging, unlike in T1, fatty tissues are dark while water is bright. The setting influencing the contrast quality is the TE echo time. It is easy to observe that if too short a TE is selected, even the transverse component with a short T_2 (which quickly dissipates) will not manage to dissipate sufficiently to make a clearly visible difference between the signal it generates and signals generated by transverse components of other tissues. For T2 weighted images, a good contrast is obtained if the TR and TE times are long.

The third type of contrasting is the proton density weighing (PD). This is based on differences in the density of protons (hydrogen atomic nuclei) in different tissues and disregards the differences in relaxation times of particular tissue types. In order to fulfill the last condition, you set a long TR repetition time and a short TE echo time. The long TR allows the $\mathbf{M_z}$ longitudinal components of both fat and areas dominated by water (taking those two extreme examples) to recover before another stimulating impulse is emitted. This mitigates the effect described above which is used for T1 imaging. Setting a short TE time after which the signal is read guarantees that the dissipation of $\mathbf{M_\perp}$ transverse magnetization components of various tissues will be practically the same. If so, then the only factor determining the signal strength ($\mathbf{M_\perp}$ length) is quantity of protons whose $\mathbf{m}$ magnetic moments contribute to $\mathbf{M,}$ which is proportional to the density. The more protons in a given tissue, the greater its $\mathbf{M}$ magnetization, the stronger the signal and the brighter the image.

Figure 2.36 shows example images of brain structures made using T1, T2 and PD contrasting.

Fig. 2.36. The same brain image made with different contrasts (from the left) T1, T2 and PD

Magnetic resonance is used particularly in the clinical diagnostics of the central nervous system, but examinations of the head and spine are also made. An MR examination of the head allows the brain tissue to be assessed, as the white matter and the grey matter (cerebral cortex), deep structures, the ventricle system, and intracranial sections of cranial nerves can be distinguished. Since there are no bone artifacts typical for the computed tomography of the head, an MR examination is the main method for assessing the structures of the posterior cranial cavity, with particular emphasis on the pons and the medulla (Fig. 2.37).
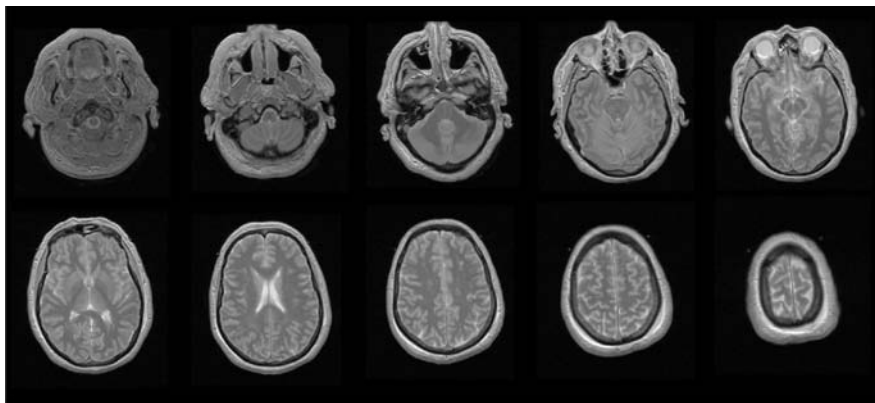

Fig. 2.37. An example NMR image of the brain

A magnetic resonance examination also makes it possible to distinguish all the main elements of the spine, including vertebral bodies and arches as well as the contents of the spinal canal. Magnetic resonance is the only method allowing the spinal cord to be directly imaged. It is worth noting that the NMR technique also allows the image of the blood flowing through arteries and veins to be visualised. Some methods of imaging require no contrast media to

be administered. Such solutions are used to examine cartoid arteries upstream of the brain and to assess intracranial arteries or veins.

Magnetic resonance is also used for examining joints, both large ones like knees, shoulders, hips or ankles, and small one like those in the wrist, palm and instep.

During the early clinical applications of magnetic resonance, it was difficult to assess of organs in the abdominal cavity due to the presence of mobile artifacts, for example caused by breathing or peristaltic movements of the intestines. The modern, fast MR apparatuses that allow examinations to be made on a held breath or feature a breath gating function for longer sequences have significantly reduced breathing-related distortions of the image. Consequently, organs from the abdominal cavity, including the liver, pancreas, spleen and kidneys, can now be assessed using magnetic resonance.

Two-dimensional MR images are usually 256×256 pixels in size or larger, whereas the depth of brightness is defined with 16 bits. If a CT and an NMR image of the same organ (Fig. 2.38) are compared, the CT scan shows more anatomical details, while the NMR image differentiates tissues of different biological functions better.

The primary advantage of NMR images is that in these images, healthy tissue can easily be told apart from diseased areas. For example, Figure 2.38 shows the NMR image of a cyst in the brain (on the left), and on the right side of the same image, a brain tumor area can easily be seen. Even a poorly experienced observer can see signs of pathology in these images. To compare, it is worth looking at Figure 2.37, which will help less experienced readers to see what the corresponding image without disease symptoms looks like.
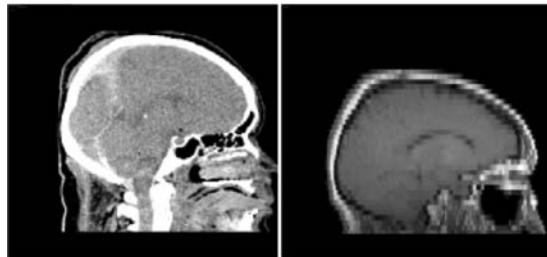

Fig. 2.38. Comparing a CT (left) and NMR (right)

When there is a good technique for imaging the anatomy of an organ (computed tomography) and there are also separate, good methods for imaging this organ clearly distinguishing functional and disfunctional features of tissues, it seems obvious and natural to combine these two images so as to get an image presenting both complete morphological information (from the CT) and information on the detected pathology (from the NMR e.g Fig 2.39).
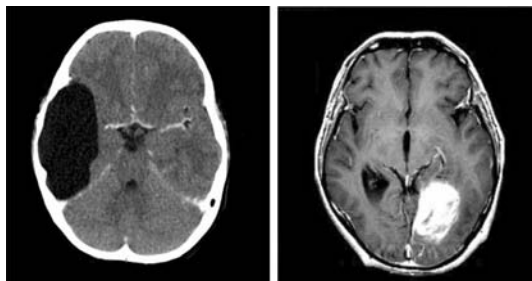
Fig. 2.39. Brain pathologies detected by NMR examinations

This idea is possible, but unfortunately difficult to put into practice. The opportunities for and methods of creating such hybrid images will be discussed in one of the subsequent chapters.

2.4. Nuclear imaging

The NMR technique described above was based on the fact that the appropriate manipulation of the magnetic field caused nuclei of atoms making up the examined tissues and organs to emit a signal. Radionuclide imaging techniques which we are going to discuss now use the fact that nuclei of isotopes of biologically active elements spontaneously emit radiation which can be recorded by modern apparatuses. The intensity of the radiation is recorded continuously together with the location from which the radiation comes (i.e. indicating the fragment of the organ in which the isotope accumulated). This allows you to follow the presence of the radionuclide, changing over time, in specific locations of the body, the route it takes to reach particular organs, the method of its excretion and the like. We should add, even if this is generally known, that a radioactive isotope undergoes chemical reactions exactly like its non-radioactive, biologically-active equivalent. So if an organ absorbs, accumulates or excretes a given chemical compound, it will do so also if the compound contains a radionuclide. However, an isotope-labeled compound can be located using apparatuses external to the patient's body, even in trace amounts. What is more, the apparatus can follow the quantity of the isotope-labeled substance in different parts of the body on a current basis. All these observations give physicians valuable information, completely inaccessible by any other means.

The key to using the above method is the availability of isotope-labeled, biologically active substances produced by pharmaceutical companies which specialize in such operations. Examples of radionuclides used in medicine with the organs for whose examination they can be used are presented in the tables in Fig. 2.40.

Fig. 2.40. Examples of radioactive isotopes used in nuclear medicine (source Internet)

It is worth calming a concern frequent among both patients and physicians by saying that radionuclides used in nuclear medicine, if properly selected and carefully examined for their radioactivity level, constitute practically no threat to the health and life of both patients and the personnel. From the patient's point of view, the dose of ionizing radiation he/she receives during a properly conducted isotope examination is lower than the dose to which his/her body is exposed during a typical X-ray.

Medical staff who come into contact with isotopes again and again (unlike the patient, who is usually exposed to them only once), must exercise some caution as even small doses of radiation can accumulate in the body. However, if the appropriate procedures are followed, there is no health hazard.

The procedure of an examination with the use of radionuclides may differ depending on the organ to be examined. For some, it is enough to drink the isotope-containing pharmaceutical in the form of a solution, other such pharmaceuticals are gaseous and can be breathed in, however the most commonplace is an intravenously injected pharmaceutical. After the pharmaceutical is administered, the patient is placed in the field of view of a gamma camera, which follows and records the path taken by the isotope in the body, and in particular the locations where it is accumulated (Fig. 2.41).

Fig. 2.41. Radionuclide examination. Radioactive pharmaceutical administration on the left, tracing its path in the patient's body on the right (source Internet)

As this book discusses mainly the techniques for medical imaging and computer processing of images, we will focus on apparatuses recording images and the properties of those images, while the physics of isotopes and the design of radiation detectors will be omitted.

The operating principle of the technique for radionuclide imaging can easily be discussed by referring to the diagram of the apparatus used by the pioneer of this examination method, **Ben Classen,** in 1950 (Fig. 2.42).
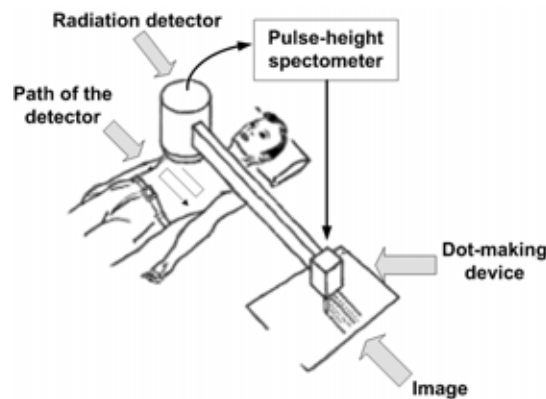

Fig. 2.42. The historical (currently abandoned) method of imaging radionuclide distribution in the human body

In the above examination method, after administering the radionuclide to the patient, a radiation detector was moved above his/her body and places where the detector measured higher radiation were marked on paper. The resultant paper map showed where there was a lot of the radionuclide, and where little. Nowadays, the same purpose is achieved easier, faster and more effectively with devices called gamma cameras (Fig. 2.43).
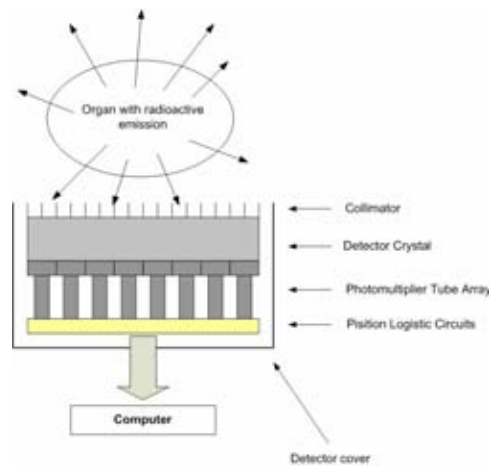

Fig. 2.43. A simplified design diagram of a gamma camera

These devices, which make use of many independent detectors (frequently equipped with photomultipliers to raise their sensitivity), can receive the radiation emitted by radioactive isotopes in tissues and organs from many points at the same time. This is illustrated (schematically and at a great simplification) in Figure 2.44, which also shows some other elements incorporated in the set of apparatuses designed for this type of examinations.
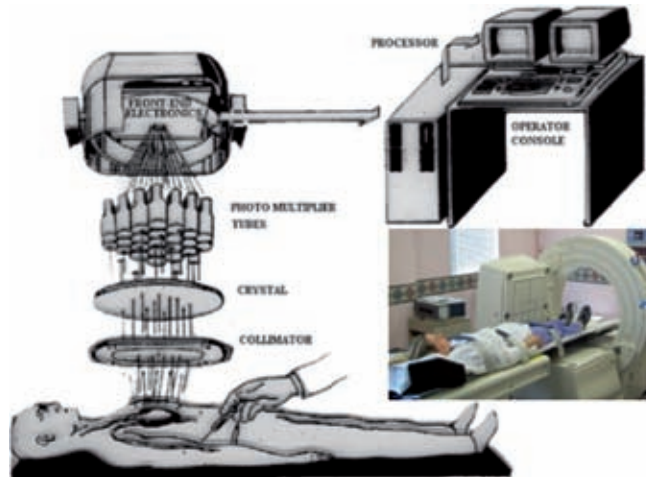

Fig. 2.44. The diagram and the appearance of a typical apparatus set for radionuclide image diagnostics (source Internet)

It is worth noting that a gamma camera, which receives very weak radiation from inside the patient's body, must be shielded very well from radiation from other sources, of which there are very many all around us. This is why the gamma camera is armored with a thick screen usually made of lead, which makes it very heavy and requires very strong equipment to transport it over the patient's body. This is obvious from the color insert in Fig. 2.44, which shows the complete example of an apparatus of the type discussed here.

Regardless of the huge weight of the gamma camera, diagnostic devices capable of receiving images from many different directions are now available: Fig. 2.45. This helps in formulating conclusions on the activity of particular parts of human organs assessed based on the distribution of the density of radioactive substances in them. This in turn makes it possible to precisely determine the location of the hypo- or hyperfunction of a specific organ, which is usually referred to as a cold or a hot artifact.

Unfortunately, the image obtained from a gamma camera is generally not very sharp, as the system of collimators determining from where the recorded radiation came cannot attempt to reach the precision of computed tomography or even an ordinary X-ray. However, if the image is properly filtered (see Fig. 2.46), it can be interpreted by a physician and can form the basis of a good diagnosis.
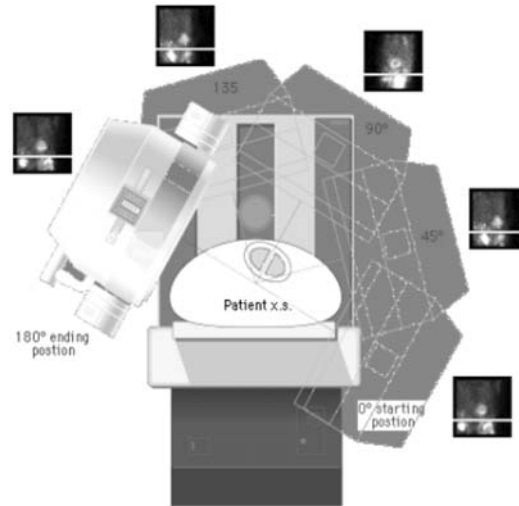
Fig. 2.45. Gamma camera ability to record images from various angles (source Internet)

The organs which are examined using radionuclides (and are the source of the type of images discussed here) mainly include: the thyroid gland (examinations of iodine uptake and metabolism), the heart (the flow of a radionuclide labeled blood allows the degree of ventricle and atrium filling of both parts of the heart to be followed), bones (the skeletal elements in which bone tissue building processes occur, and which are sometimes connected with tumors, can be observed), kidneys (excretion of radioiodinated hipuran) and many others.
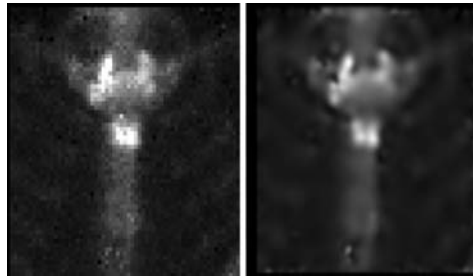

Fig. 2.46. Image from a gamma camera. Unprocessed on the left, filtered on the right

A particularly useful feature of radionuclide examination is that the images produced show not just the static distribution of the concentration of the substance labeled with the radionuclide which is followed in particular parts of the organ, but also the process of accumulating and expulsing that substance from various organs over time (Fig. 2.47). This forms a very valuable source of diagnostic information, which is completely inaccessible in any other way.
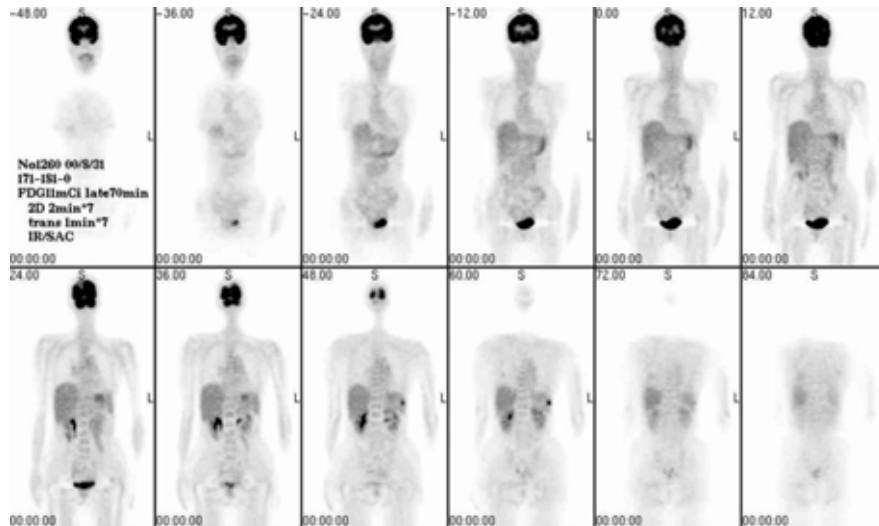
Fig. 2.47. The image of radionuclide distribution within the patient's body, changing over time (source Internet)

2.5. PET imaging

Another modern imaging method called PET (Positron Emission Tomography) is also a radionuclide technique, so in theory it could (or even should) be discussed in the previous chapter. However, as it has many specific characteristics, PET imaging is usually treated as a separate subject, and we will follow that convention in our book [25].

Nowadays, PET is replacing the older and worse technique called SPECT (Single Photon Emission Computed Tomography). PET offers a much better spatial resolution than SPECT and allows one to examine biological events which run much faster. PET makes use of isotopes of much shorter "life", e.g. ^{15}O, ^{13}N and ^{11}C whose half-lifes range from 2 to 20 minutes. Compare this to SPECT, which uses the ^{99m}Tc and ^{127}Xe isotopes with the half-life of 6 hours. This means that a patient undergoing PET examination is examined more precisely and also receives a smaller dose of the harmful radiation. Unfortunately, PET also has a disadvantage: it is extremely expensive!

A diagram of a PET examination is shown in Fig. 2.48. The patient is given a pharmaceutical labeled with a radionuclide of a very short lifetime which for that very reason (as it decays very quickly) cannot be bought for stock, but has to be produced right before the examination in a cyclotron, which forms a part of the PET apparatus set. The interaction between the highly-energetic gamma rays emitted by the isotope and the matter of the human body, causes positrons to be

emitted, whose subsequent annihilation is accompanied by the emission of two gamma quanta with the energy of 0.511 MeV in two opposite directions. These events are recorded by a set of detectors distributed around the patient, Fig. 2.49.
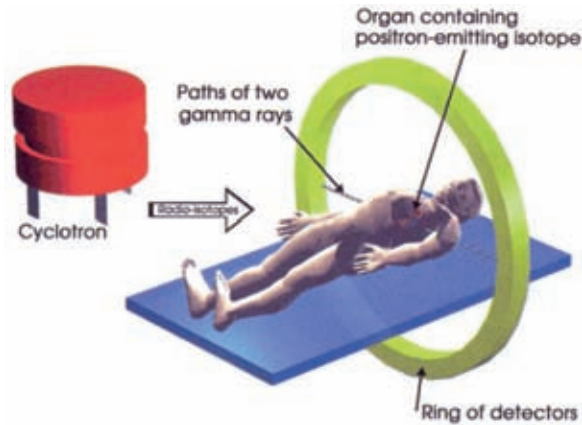

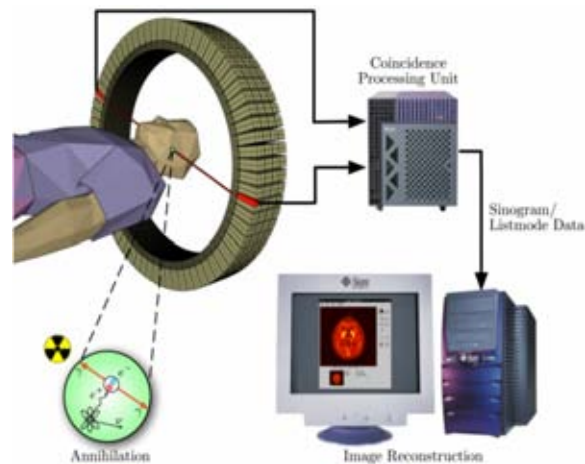**Fig. 2.48.** A diagram of a PET imaging apparatus (source Internet)

Fig. 2.49. The method of locating the part of the patient's body containing the active atom by capturing the coincidence of two gamma quanta in the ring of detectors (source Internet)

The main advantage of the PET examination is that if fluorodeoxyglucose (FDG) is used to carry the short half-life isotope (fluorine ^{18}F) (Fig. 2.50), the compound ends up in places which at that moment exhibit an increased energy demand, i.e. in areas which are highly active. As the presence and concentration of FDG can be detected with the PET apparatus, it offers an unequalled opportunity to follow the activity of particular organs (mainly the brain).
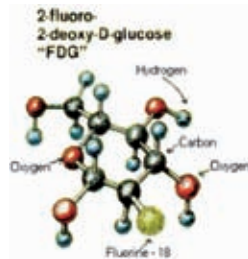
Fig. 2.50. FDG (fluorodeoxyglucose) labeled with the ^{18}F fluorine isotope

A convenient way to follow this is on a series of images showing PET scans of the brain of the same person in four situations: when he/she is intellectually and sensorially inactive (Fig. 2.51), when he/she is solving a math problem (Fig. 2.52), when he/she is watching an interesting picture (Fig. 2.53) and when he/she is listening to a conversation (Fig. 2.54).
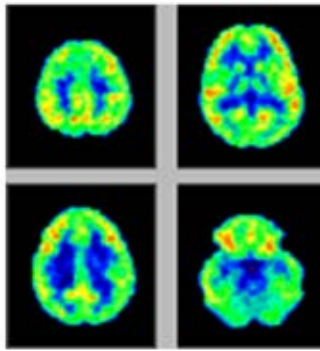

Fig. 2.51. Image of the brain of an awake person who is not concentrating on any specific activity
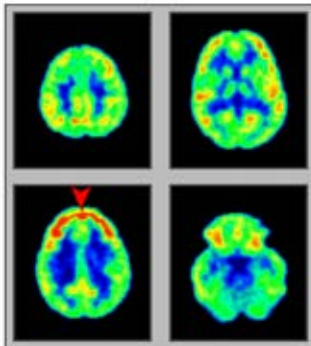

Fig. 2.52. Image of the brain activity of a person solving a difficult math problem. The strong, red color of frontal lobes (indicated by the arrow) shows their activity
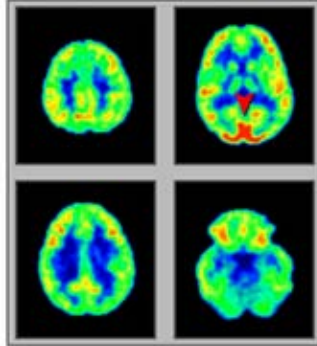
Fig. 2.53. The brain activity of a person watching an interesting scene. A visible activity of occipital lobes which are responsible for receiving and recognizing vision information
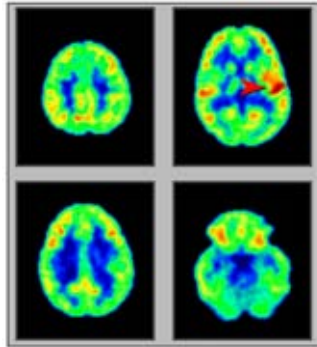

Fig. 2.54. In someone listening to a conversation, activity concentrates in temporal which contain the centers for sound reception and analysis. It is worth noting that temporal areas are active only on one side, as the speech decoding functions are located in only one cerebral hemisphere. If this person were listening to music, both temporal lobes of the brain would "light up".

PET images allow you to record not just the changes in the healthy brain activity connected with the performance of specific activities, but the symptoms of various diseases, as they are very clearly visible in this imaging (Fig. 2.55).
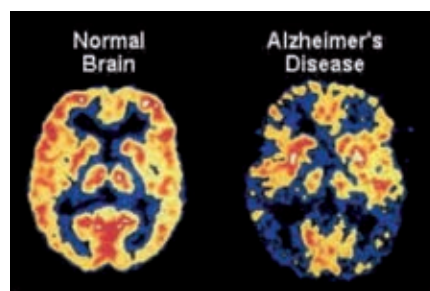

Fig. 2.55. PET images allow lesions to be imaged precisely

One advantage of PET images is that they help to examine the activity of many organs and thus to collect diagnostic information which cannot be acquired in any other way. On the other hand, their shortcoming, obvious in Fig. 2.51–2.54, is the poor resolution for presenting anatomic details. This is why attempts are frequently made to combine the PET image (showing dysfunction locations) with the image from ordinary computed tomography (CT), to get an image rich in both morphological information (identifiable anatomic details, useful for planning and controlling neurosurgical procedures) and in functional information from PET imaging. However, this combination of images is made difficult by problems with the automatic assignment of corresponding fragments of both overlaid images. This is because the CT and PET examinations are made using different apparatuses and at different times, so one cannot expect their cross-section planes to be identical in both images. In addition, both examinations yield images with different resolutions, which necessitates a complex assignment of whole sets of pixels of one image to single pixels of the other. However, a successful overlaying of both images generates an image of exceptional diagnostic and therapeutic utility (Fig. 2.56).
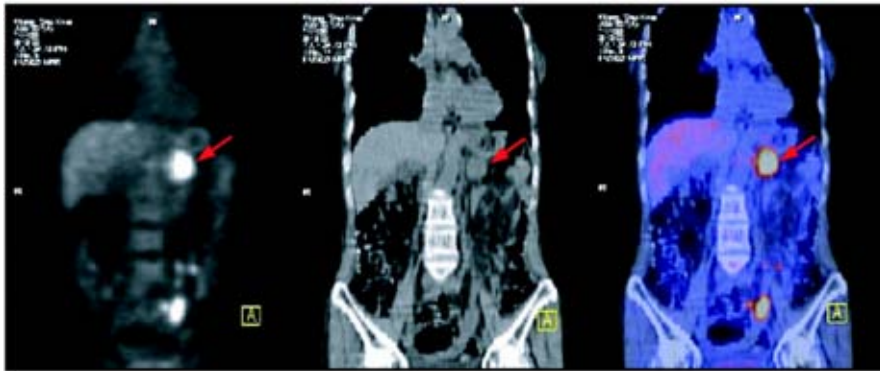

Fig. 2.56. Overlaying PET and CT images. The PET image (left) shows the places in which the function of organs is abnormal, the CT image (middle) shows anatomic details, while the combination of both images (right) gives the best grounds for drawing diagnostic conclusions

2.6. USG images

Ultrasonographic diagnostics (USG) works by emitting recording the reflections of sound waves after they penetrate through tissues and bounce back from boundaries of structures characterized by different densities ρ and different velocities of sound-wave propagation (Fig. 2.57). A short ultrasound impulse sent by the transducer (on the left) propagates through the tissue with the density of ρ_1 and the sound-wave propagation velocity of c_1 and then reaches an organ whose tissues

have density ρ_2 and sound-wave propagation velocity c_2. At the boundary between these structures, some of the ultrasound wave is reflected and returns to the ultrasound transducer, creating an echo [4, 5].
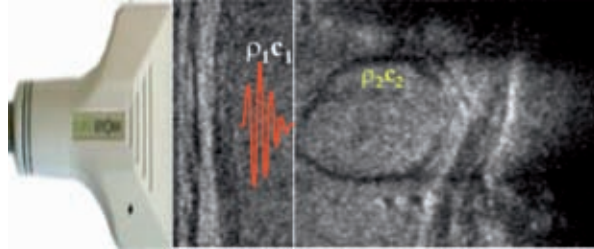

Fig. 2.57. Generation of the ultrasound echo. Described in text

The proportion of the energy of the wave hitting the organ and that reflected from it is determined by the following formula:

$$R = \frac{Z_2 - Z_1}{Z_2 + Z_1} = \frac{\rho_2 c_2 - \rho_1 c_1}{\rho_2 c_2 + \rho_1 c_1}$$

Most frequently, the structures reflecting ultrasound waves are the surfaces of internal organs, whose contours can therefore be detected and located, although sometimes there are reflections from elements within the examined organ which are not distinguished by anything else, producing interference and distortions in the image. The diagram of an USG apparatus is shown in Fig. 2.58.
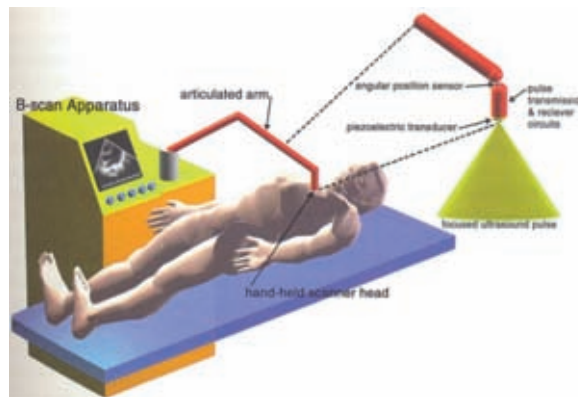

Fig. 2.58. A diagram of the USG apparatus design (source Internet)

The velocities of ultrasound waves in various media are shown in the table 2.1.

Table 2.1. Velocities of ultrasound waves in various media

Substance	Velocity [m/s]
air	340
blood	1,570
bone	2,500 – 4,700
fat	1,450
brain	1,540
liver	1,550
kidney	1,560
spleen	1,578
water	1,530

What is notable is the very large difference in the velocity at which ultrasounds travel through the air and through body tissues. If a layer of air remained between the ultrasound transducer and the patient's skin, 90% of the wave energy would be reflected and would not penetrate the body. This is why, during the examination, the contact between the transducer and the patient's body is so crucial, so to secure it a special gel or water-filled plastic bags are used.
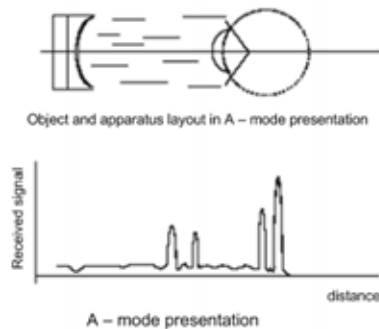
Fig. 2.59. The A presentation of USG examination results

In some cases, immersion examination is conducted in a water bath. All these measures aim at eliminating even the smallest air bubbles from the space between the transducer and the patient's body, as those could disturb the read-out. An alternative examination is intra-operative ultrasonography, done during surgical procedures. This consists in sliding a sterile transducer directly over the examined

organ and is very useful in searching for stones in gall ducts or kidneys and for assessing the cancer process [4, 5].

There are several methods for imaging internal organs with the use of the USG. We will discuss them in sequence, indicating their possible uses and the problems connected with the computer transformation of these images.

- The A-mode (Amplitude) presentation is the oldest imaging method in which the piezoelectric transducer generated only short impulses. The whole apparatus operated as an ultrasound echoscope. The echoes of reflected waves, after their amplification in the receiver, were transmitted to the vertical deflection systems of an oscilloscope tube. The time until the echo return was presented on the horizontal axis, which could be calibrated as the scale of the distance from the transducer based on the known ultrasound propagation velocity. A line was plotted above that time/distance axis, and its vertical deflections corresponded to the location of structures reflecting the ultrasound wave (Fig. 2.59). The measurement of the time passing between the return of subsequent echoes was used to determine the position and dimensions of the organs examined (Fig. 2.60). The A-mode presentation had its specific advantages. Experienced physicians (diagnosticians) could determine, on the basis of the slope of the rise and fall of the echo wave, the characteristics of the tissues from which the wave bounced. However, in general, that method provided little information and has since been almost completely discontinued. This examination is only used in a few areas of medicine, including ophthalmology.
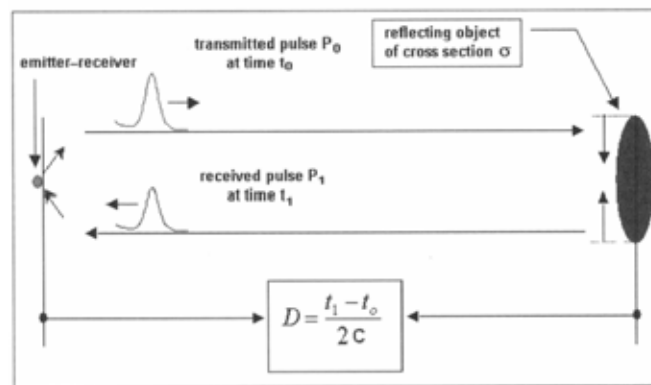

Fig. 2.60. Methods of measuring the location and dimensions of objects in USG examinations

- The B-mode (Brightness) presentation consists in displaying a two-dimensional cross-section of the examined part of the body (e.g. the abdominal cavity) in which the momentary value of the received signal modulates the brightness of subsequent image points. This is based on transforming the amplitude of echoes received from the direction in which the ultrasound beam is propagated into the brightness with which dots shine, as a result of which the monitor shows a

line of various brightness. If the ultrasound transceiver is slid and another impulse is sent, the brightened dots will plot another echo line on the monitor. Their character corresponds to the acoustic properties of the part of the organ which is probed with the subsequent ultrasound beam. By repeating this process frequently enough, e.g. by shifting the beam by a distance corresponding to that between adjacent pixels of the monitor (usually the beam is shifted by a distance of several pixels), you get a two-dimensional picture made up of nearby lines of modulated brightness. The structure of the layout of lines making up the B image is usually a fan, due to the design of modern transceivers which usually transmit and receive many ultrasound beams at the same time.

Fig. 2.61. Example of a B-mode sonogram (source Internet)

This technique is frequently used to examine stationary organs. In this method, ultrasound echoes are displayed on the monitor in such a way that they make up a picture of the geometric outline of the examined organ. As the brightness of the dot is proportional to the amplitude of the reflected wave, the organs examined are called more or less echogenic, which term derives from this technique. The horizontal dimension of the dot depends on the width of the echo at its base. The bigger the echo, the brighter the dot. B-mode USG images are usually saved with the resolution of 700×500 pixels or lower and a brightness depth represented with 8 bits. An example image obtained by the B-mode presentation is shown in Fig. 2.61. By superposing a number of B-mode images one over the other using a computer, a 3D image of a very realistic appearance (Fig. 2.62) can be obtained, which is frequently very useful, although by no means necessary for the diagnostic suitability of the image.

Fig. 2.62. A 3D reconstruction of an object (the fetus's head in its mother's womb) obtained by a computer processing of a B-mode presentation

- **M**-mode (**M**otion) presentation, formerly called **TM** (**T**ime **M**otion), consists in listening to the echo from the same direction at two subsequent moments. The echoes are displayed as in the B-mode, which means that the momentary value of the signal modulates the brightness of the dots displayed, and subsequent lines are drawn vertically side by side. In this option, the time base of the oscilloscopic tube brightens only in the places where ultrasound echoes appear. Echoes coming from mobile organs are represented on the time base by mobile bright dots, which leave a trace on the screen. The M-mode presentation is still fundamental in examining the function and imaging the structure of the heart (Fig. 2.63). Its other uses include imaging the abdominal aorta, and in particular its aneurisms.
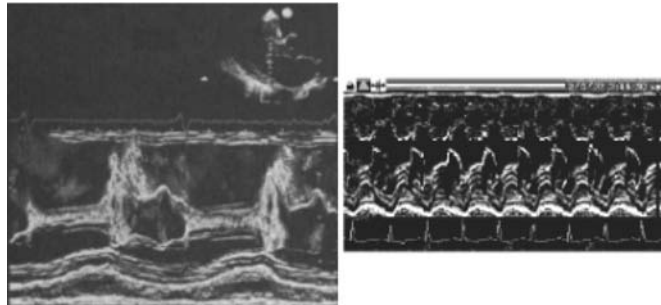

Fig. 2.63. An M-mode USG image

- The **D-**mode (**D**oppler) consists in receiving the USG wave dispersed by the moving blood cells, which returns to the transceiver with a changed frequency (the Doppler effect). Depending on the velocity and direction of blood cell motion relative to the USG beam and the direction in which the wave is propagated, there is a Doppler shift of the frequency of the sent and received wave towards higher or lower frequencies. On the image, this is usually shown in color: blue for the fastest movement in one direction, and red for the fastest motion in the opposite direction. Intermediate colors code movements at lower velocities, while the echoes coming from stationary structures are presented as black-and-white. An example of a very beautiful D-mode image is shown in Fig. 2.64. It presents the umbilical cord of a fetus.

Fig. 2.64. An image obtained by D-mode presentation

Obviously, the umbilical cord channels the flow in two directions, as the intertwined blood vessels transport blood to and from the placenta – which is very clear in the image. The D-mode presentation is used to diagnose the blood flow, one purpose of which can be to locate narrowings of blood vessels, and therefore constitutes a key diagnostic tool in modern cardiology. The technique has the following varieties:

– The **CFM-mode** (Color Flow Mapping) presentation consists in filling a sector of the B-mode black-and-white image selected by the operator with a color image of the flows measured using the correlation technique.
– The **CFA-mode** (Color Flow Angiography) consists in identifying the flow, assigning a color to the areas in which the flow has been identified and incorporating them in the black and white B-mode image.
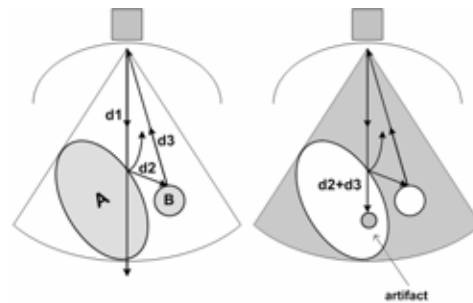

Fig. 2.65. Creating artifacts in a USG image

The USG image may be subject to much more noises and deformations that other medical images described previously here. There are many causes of deformations. The simplest one is called specles. This is a non-uniform structure of the ultrasonographic image caused by the local interference of waves reflected within the medium. Specles look like randomly distributed black and grey spots on the bright image background. They depend on the non-uniformity of the medium and the magnitude of impulses probing it. Another source of noise consists of the different velocities at which ultrasound travels through layers of tissues which make it difficult to precisely scale the dimensions of the examined structures. As we know, the USG apparatus measures the differences in the return time of the echo bouncing from different structures and presents them on the image under the assumption that the distance traveled by the impulse over a unit of time is the same in every place, which is obviously untrue. What is more, the surfaces between environments of various ultrasound propagation velocities not only reflect waves (which is necessary to obtain the image), but also refract them. As a result, the probing impulses, instead of traveling down straight lines along the direction of the beam produced, which is assumed when generating the USG image, follow an indeterminate, winding and complicated route, which can only be roughly approximated as a straight line. The dampening of the energy of the wave penetrating tissues weakens the echoes returning from deeper structures, as a result of

which the image is darker behind structures which reflect a lot (an acoustic shadow appears). All the above phenomena disturb the image and cause artifacts to appear – Fig. 2.65. Artifacts appear in the USG image as the echoes of objects which:

1. Do not really exist (multiple reflections);
2. Are represented in the wrong location (multiple reflections, wave refraction);
3. Are of deformed dimensions, shape and brightness (wave refraction, phase aberration, various sound velocities).

The majority of artifacts are caused by the physical properties of wave propagation through tissues, but some are caused by the incorrect setting of the apparatus, mainly the amplification, the range adjustment of amplification as well as the pre- and post-processing functions selected [4, 5].